Article:
Ukpata, JO, Basheer, PAM and Black, L orcid.org/0000-0001-8531-4989 (2019) Expansion of CEM I and slag-blended cement mortars exposed to combined chloride-sulphate environments. Cement and Concrete Research, 123. 105794. ISSN 0008-8846

https://doi.org/10.1016/j.cemconres.2019.105794

Expansion of CEM I and slag-blended cement mortars exposed to combined chloride-sulphate environments

Joseph O. Ukpata[1,2], P. A. M. Basheer[2] and Leon Black[2]

[1.] Department of Civil Engineering, Cross River University of Technology, Calabar, Nigeria

[2.] School of Civil Engineering, University of Leeds, Leeds, United Kingdom

Abstract

This study investigates the effects of specimen curing duration, temperature, and slag composition on expansion of CEM I and composite slag-cement mortars exposed to a combined NaCl and Na_2SO_4 solution for up to 664 days. Test prisms prepared at 0.5 w/b ratio, were wet-cured for either 7 or 28 days prior to submersion in a combined salt solution at temperatures of 20 or 38℃, to simulate temperate or warm tropical climates respectively. Equivalent reference specimens were stored in saturated limewater at 20℃ and tested in parallel. Mortar samples were used to investigate expansion and sorptivity, while corresponding paste specimens were prepared, cured and exposed under similar conditions for chemical and microstructural investigation. Such characterisation was performed on specimens immediately prior to exposure to salt solution and after the onset of expansion. The results show significant resistance to sulphate-induced expansion for specimens cured and exposed at 38℃. For slag blends, the influence of exposure temperature was found to be more pronounced than curing duration. Differences in slag composition and curing duration also played key roles on the expansion resistance of mortar specimens. Expansion was attributed to the formation of ettringite crystals due to the reaction of aluminate phases of the binders with sulphate ions, although Friedel's salt and Kuzel's salt were also formed. The presence of chloride mitigated sulphate expansion of CEM I. For slag blends, it was shown that sulphate expansion was significantly reduced with increasing slag contents.

Keywords: slag, cement, expansion. Chloride, sulphate

1.0 Introduction

Sulphate attack is a concern for concrete durability wherever concrete may come into contact with sulphate ions, potentially leading to expansion, cracking and spalling of mortars and concretes. A number of hypotheses have been given to explain the mechanisms of expansion of cement systems due to sulphate attack [1, 2]. The most acceptable hypothesis is related to crystallization pressure theory [3-7]. This relates expansion to pressures due to the formation of ettringite crystals from pore solutions which have been supersaturated with respect to ettringite, following continuous ingress of sulphate ions. Such crystals growing in confined pore spaces exert expansive forces on the pore walls leading to expansion. Yu et al. [5] explained that the penetrated sulphate ions first react with monosulphate, buffering any increase of sulphate ions in the pore solution until all transformable alumina had been used. Then, the concentration of sulphate in the pore solution would increase and become oversaturated, which triggers its reaction with monosulphate, leading to ettringite precipitation within the hardened cement paste. According to Müllauer et al. [8], expansion and degradation in mortar specimens occurred when the stresses generated (approximately 8 MPa) due to

ettringite formation in small pores (10-50 nm) had exceeded the tensile strength of the binder matrix (3-4 MPa).

Further work by Yu et al. [9] differentiated sulphate-oriented degradation between CEM I and slag-blended cement mortars. It was reported that CEM I showed initial generalised slow expansion, followed by rapid increase in expansion up to failure. For the slag blends, however, expansion was not generalised due to limited penetration of sulphate solution. Hence, damage was localized and occurred in stages from the surface region and increasing to greater depths, as damage in the outer region allowed further ingress of sulphate ions into deeper sections. Slag blends are generally known to be more resistant to sulphate attack than plain CEM I due to the buffering role of their more refined pore structure [10-15]. It has also been reported that the formation of both monocarboaluminate and ettringite due to the addition of limestone reduced sulphate attack in slag blends [13]. Also, Kunther et al. [16] found that sulphate expansion in mortar specimens was reduced in blends with lower Ca/Si ratios of the C-S-H, such as is observed in slag blends. This behaviour was attributed to decreased supersaturation of the pore solution with respect to ettringite caused by leaching and decalcification of C-S-H and portlandite. Furthermore, decreased C_3A content in cement is known to lessen the effects of sulphate attack [17, 18]. No significant difference in expansion was observed due to changes in attacking sulphate concentration, although damage was found to increase as sulphate concentration was increased from 3 to 30g/l [9].

In addition to their presence in groundwater, sulphates present in seawater are a major concern for concrete durability [19]. In seawater, sulphate ions are naturally present along with other anions, typically, chlorides and the investigation of sulphate attack is thus more plausible using combined solutions. The influence of chloride on sulphate attack is still controversial and depends on many factors, including the nature of attacking sulphate ions and environmental conditions. Many researchers have reported on the mitigating role of chlorides on sulphate attack [19-22]. However, others have found neither positive nor negative effects of chlorides when sodium is the cation [10], but an aggravating effect when magnesium is the cation [23]. Also, there are indications that the mitigating effect of chloride on sulphate attack could be more significant in CEM I than slag cements [24, 25], because the alumina in slags do not react directly with incoming sulphate ions to form ettringite but are bound in C-S-H, monosulphate and hydrotalcite during the hydration of slag [1].

The dependence of sulphate attack on temperature and binder type has also been studied [23]. However, differences in cement materials and the investigated temperature ranges in the literature have left gaps and conflicting findings, necessitating further investigation. Hossack and Thomas [26] studied the effect of temperatures between 1 and 23℃ on Portland cement blended cements, with resistance to external sulphate attack of the blended cements improving with increasing temperature. Similarly, Maes and de Belle [23] looked at CEM I, sulphate resisting cement and a 50% cement-PC slag blend and found that chlorides did not affect magnesium sulphate damage for CEM I and sulphate resistant cement at 20℃, but that there was increased degradation for the slag blend at 5℃. There appears to have been more emphasis on the effects of low temperatures, likely due to concerns over the thaumasite form of sulphate attack, where temperatures below 15°C are associated with thaumasite formation [12, 23, 27-31]. Investigations into performance at higher temperatures are less common. Although, it was reported that raising temperature of exposure solution from 20 to 40℃ did not accelerate sulphate attack [32]. Conversely, Santhanam et al. [33] found that expansion of PC mortars increased with increasing temperature and sulphate concentration. Given the contradictory nature of the literature, the present study investigates the influence of elevated temperature, curing duration and binder type or slag composition, on external sulphate attack from combined chloride-sulphate solutions.

2.0 Experimental details

2.1 Materials and specimen preparations

Two slags of different basicity ratios (CaO + MgO)/SiO_2) = 1.28 & 1.18)), designated as slags 1 and 2, were each blended with CEM I 52.5 R to produce 30 wt.% slag blends. These slag blends were used in this study, together with a plain CEM I 42.5 R. This approach reflects industrial practice where composite cements can often be blended with a slightly finer clinker. The chemical and physical properties of the cements and slag are as previously reported [34], but are presented in Tables 1 and 2 for completeness. The particle size distributions were similar for the binders. Fine aggregate used for mortar specimens was natural siliceous sand sieved to 2.0mm maximum particle size. Mortar prisms (25x25x200mm) for expansion tests were cast in steel moulds at 0.5 w/b ratio (Table 3) and cured at either 20℃ or 38℃ for 7 or 28 days. The natural water content of the fine aggregate prior to mixing was 0.81%, while the water absorption was 2.26%, giving an effective w/b ratio of 0.493. The specimens were then soaked for 24 hours in deionised water before immersion in a combined NaCl (30g/l) and Na_2SO_4 (3g/l) solution at either 20℃ or 38℃ for up to 66 4 days. The concentrations of chloride and sulphate were similar to those in typical seawater, and also chosen to replicate those used in similar earlier studies looking at chloride [35] and sulphate [11] attack. The liquid to solid ratio was approximately 4. The test solution was renewed monthly. Parallel specimens were immersed in lime water for reference measurements.

Microstructural development and the development of the phase assemblages were followed by preparing paste specimens of identical binder composition to the mortar samples. Pastes were mixed by hand for 3 minutes before being poured into ∅14 x 50 mm plastic vials. The lids were closed and sealed before the vials were rotated for 24 hours to prevent bleeding. Samples were then placed in plastic bags, vacuum sealed and placed in water baths at either 20 or 38°C for either 7 or 28 days before demoulding and exposure to the salt solution. Specimens were then taken from the centre of the paste specimens at different ages (i.e. 7, 28 and 180 days), to mark the periods just before exposure to the combined salt solution and after the onset of significant expansion.

Table 1: Chemical compositions of cementitious materials (As received)

Component	Unit	CEM I 42.5R (C1)	CEM I 52.5R (C2)	Slag 1 (S1)	Slag 2 (S2)
SiO_2	%	20.17	20.50	36.58	40.14
Al_2O_3	%	5.33	5.43	12.23	7.77
TiO_2	%	0.29	0.29	0.83	0.30
MnO	%	0.05	0.05	0.64	0.64
Fe_2O_3	%	2.65	2.51	0.48	0.78
CaO	%	63.01	63.43	38.24	37.90
MgO	%	1.45	1.51	8.55	9.51
K_2O	%	0.76	0.79	0.65	0.55
Na_2O	%	0.14	0.17	0.27	0.36
SO_3	%	3.33	3.43	1.00	1.47
P_2O_5	%	0.12	0.14	0.06	0.02
LOI 950℃	%	2.12	1.37	1.66	0.40
Total at 950℃	%	99.42	99.62	99.88	99.43
Glass content	%	na	na	99.3	97.1

Table 2: Physical properties of cementitious materials

Property	Unit	CEM I 42.5R (C1)	CEM I 52.5R (C2)	Slag 1 (S1)	Slag 2 (S2)
Blaine	cm^2/g	3490	7357	5995	5540
Density	g/cm^3	3.14	3.16	2.93	2.91
D10	µm	3.54	2.94	2.27	2.87
D50	µm	16.29	9.43	11.56	12.91

Table 3: Mix design for mortar specimens

Binder	W/B ratio	CEM I (g)		GGBS (g)		Water (g)	Sand (g)
		42.5 R	52.5R	S1	S2		
C1	0.5	450	0	0	0	225	1350
C2S1	0.5	0	315	135	0	225	1350
C2S2	0.5	0	315	0	135	225	1350

2.2 X-ray diffraction

X-ray diffraction (XRD) was performed on bulk powder specimens, using a Bruker D2 phaser diffractometer with a Cu Kα source and 1D mode Lynxeye detector, operating at 30 KV and 10 mA. Prior to XRD analysis, specimens were hydration stopped using the isopropanol solvent replacement method. Scanning was performed from 5°to 70° 2θ, at 0.034° increment with a scan time of 2 s and specimen rotation of 15 rpm. BRUKER XRD DIFFRAC.SUITE V3.0 software was used for phase identification in conjunction with published data in the literature.

2.3 Chemically bound water from thermal analysis

Thermogravimetric analysis (TGA) was performed on hydrated paste powder specimens using a Stanton Redcroft 780 series thermal analyser. Specimens were heated at temperatures of 20℃ to 1000℃ at a constant heating rate of 20℃/mi n, under nitrogen gas at a flow rate of 50 ml/min. The initial specimen weights were kept fairly uniform at 16±1 mg. Bound water was taken as the mass loss between 50℃ and 550℃ [35]. Withi n this range of temperatures, it was assumed that all water-containing phases would have been decomposed. Bound water content (W_b) was calculated according to Equation 1.

$$W_b = \frac{(W_{50} - W_{550})}{W_{550}} x\ 100 \quad (1)$$

Where

W_b is the bound water (%);

W_{50} is the residual mass at 50℃; and

W_{550} is the residual mass at 550℃.

2.4 Degrees of hydration and capillary porosity from SEM image analysis

In order to follow the hydration of CEM I clinkers and slag blends, polished, resin-embedded paste specimens were examined by scanning electron microscopy. Thirty backscattered electron images (BSE) were randomly obtained per specimen using a Carl Zeis EVO MA 15 scanning electron microscope (SEM) at 800x magnification at working distance of 8.0-9.0mm and accelerating voltage of 20KeV. According to Scrivener et al. [36], 10-20 images were adequate for reasonable statistical accuracy, at moderate (30-40%) replacement levels. BSE images for the slag-blended paste specimens were supplemented with energy dispersive x-ray spectroscopy (EDX) The lack of magnesium mobility during hydration was exploited to determine the degree of slag hydration. Mg elemental maps were used to locate the original location of unhydrated slag, and ImageJ software was used to overlay this over BSE maps identifying slag [37]. The degree of clinker hydration at any given age was calculated according to Equation 2.

$$\alpha_{PC} = \frac{V_{anh.PC}(t=0) - V_{anh.PC}(t)}{V_{anh.PC}(t=0)} \quad (2)$$

Where:

α_{PC} = degree of hydration of CEM I (PC)

$V_{anh.\ PC}(t=0)$ = volume fraction of initial anhydrous PC

$V_{anh.\ PC}(t)$ = volume fraction of unreacted PC remaining at time t (in days).

Also, the degree of slag hydration at any given time was calculated from Equation 3, in line with [38].

$$\alpha_{slag} = \frac{V_{anh.slag}(t=0) - V_{anh.slag}(t)}{V_{anh.slag}(t=0)} \quad (3)$$

Where:

α_{slag} = degree of slag hydration

$V_{anh.\ slag}(t=0)$ = volume fraction of initial anhydrous slag

$V_{anh.\ slag}(t)$ = volume fraction of unreacted slag remaining at time t (in days).

BSE images were also analysed using ImageJ to quantify the coarse capillary porosity at 7 and 28 days. On a BSE image the pores can be identified as the darkest regions and a threshold was implemented following the method suggested by Scrivener [39] and adopted by many researchers [35, 40].

2.5 Mortar sorptivity

Sorptivity was measured using 28 mm ϕ x 50 mm cylindrical mortar specimens. The schematic of the test set-up is shown in Figure 1. The mortar specimens were conditioned to constant weight in an oven at (40 ± 2) ℃, according to BS EN 13057 [41] and later cooled to ambient

temperature (ca. 20°C). The near bottom perimeter of each specimen was coated in paraffin wax to allow only unidirectional uptake of water. Each specimen was then suspended on a stainless steel wire mesh in a tray containing deionised water at ca. 20°C, such that only about 5 mm of the specimen was submerged in water.

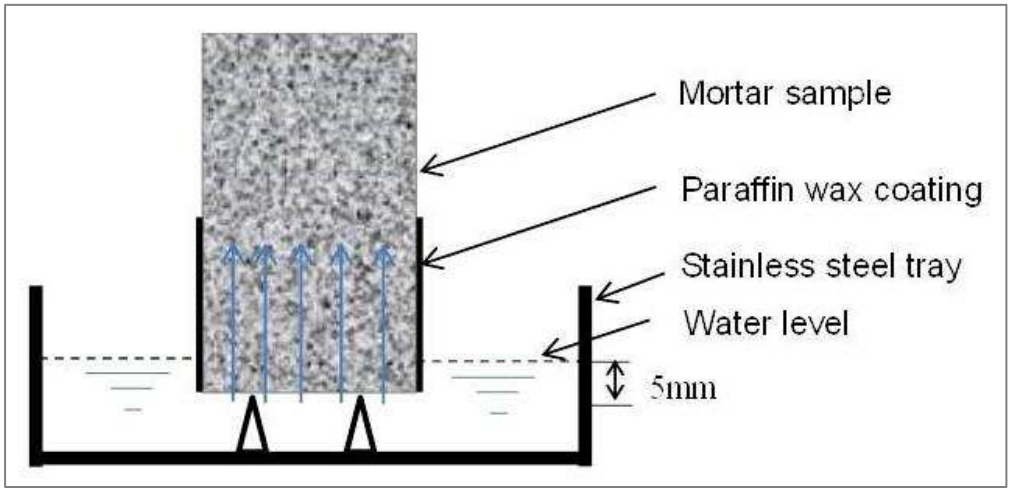

Figure. 1. Schematic set-up for measuring the rate of water absorption in mortar specimens.

The mortar masses were measured at 1, 4, 9, 16, 25, 36, 49 and 64 minutes, similar to the procedure used by other researchers [42, 43]. The sorptivity coefficient was obtained from the slope of the plot of cumulative water absorption (g/mm^2) against the square root of time (min$^{0.5}$), in line with Equation 4.

$$i = K\sqrt{t} \quad (4)$$

Where:

i = cumulative water absorption (g/mm^2),

t = time (minutes), and

k = sorptivity (g/mm^2/min$^{0.5}$).

2.6 Expansion measurements

Expansion of mortar prisms (25 x 25 x 200 mm) was measured regularly, in triplicate, using a length comparator test rig equipped with a digital dial gauge. Details of the exposure conditions are given in Table 4. Expansion measurements were made weekly for the first month, then after weeks: 8, 13, 15, 24, 36, 45, and 52, for the first year. Subsequently, regular monthly measurements were taken, up to a total exposure period of 664 days. Expansion was calculated in line with Equation 5. This approach is consistent with the literature for length change measurements in cement systems [40, 44].

$$\delta_l = \frac{(L_x - L_i)}{L_i}\, x\, 100\% \quad (5)$$

Where δ_L = length-change or expansion (%), L_x = measured length (mm) at a given period of exposure (in weeks), L_i = initial baseline measurement for the same specimen.

Table 4. Exposure conditions.

Exposure type	Initial curing	Exposure environment	Exposure temperature
X1	7 or 28 days in water	immersed in saturated lime water	20℃ or 38℃
X2	7 days in water	immersed in combined chloride-sulphate solution	20℃ or 38℃

3.0 Results and discussion

3.1 Hydration and characterisation before and after exposure to salt solution

The relative volumes of anhydrous and hydrated slag and clinker, together with the coarse capillary porosity, are presented in Figures 2 and 3, following hydration of each binder for 7 and 28 days respectively. The volumes in Figures 2 and 3 were based on the degrees of hydration (Table 5) and coarse porosities (Table 6) derived from scanning electron microscopy-image analysis (SEM-IA)). This was a slight simplification and did not account for bound water and porosity less than ~2 µm [37]. After 7 days' hydration at 20℃, the total volume of hydrated products in plain CEM I was greater than that in either of the 2 slag blends. However, this trend was reversed at 38℃ due to accelerat ed slag hydration. This change also led to lower coarse porosity in the slag blends. By 28 days, the volumes of hydration products in the slag blends were greater than those of plain CEM I irrespective of temperature. This is due to the more gradual hydration of slag, which continues over longer periods than CEM I. The coarse porosity of the specimens cured at 38℃ were still lower for slag blends than CEM I, while at 20^{o}C, it was the CEM I specimen which showed slightly lower porosity. The trends are consistent with the weighted degrees of hydration shown in Table 5, and the coarse porosity in Table 6.

It is worth comparing the data from the specimens cured for 28 days and those from the specimens cured for 7 days and then immersed in the combined salt solution for 21 days, i.e. specimens 28X2 in Tables 5 and 6. The weighted degrees of hydration were always slightly greater following immersion in the combined chloride-sulphate solution. This reflects the common knowledge that chlorides accelerate hydration of the silicate phases in clinker [45, 46] and also that sulphates can accelerate slag hydration [37, 47]. This resulted in more hydration products, thereby reducing coarse porosity as shown in Table 6.

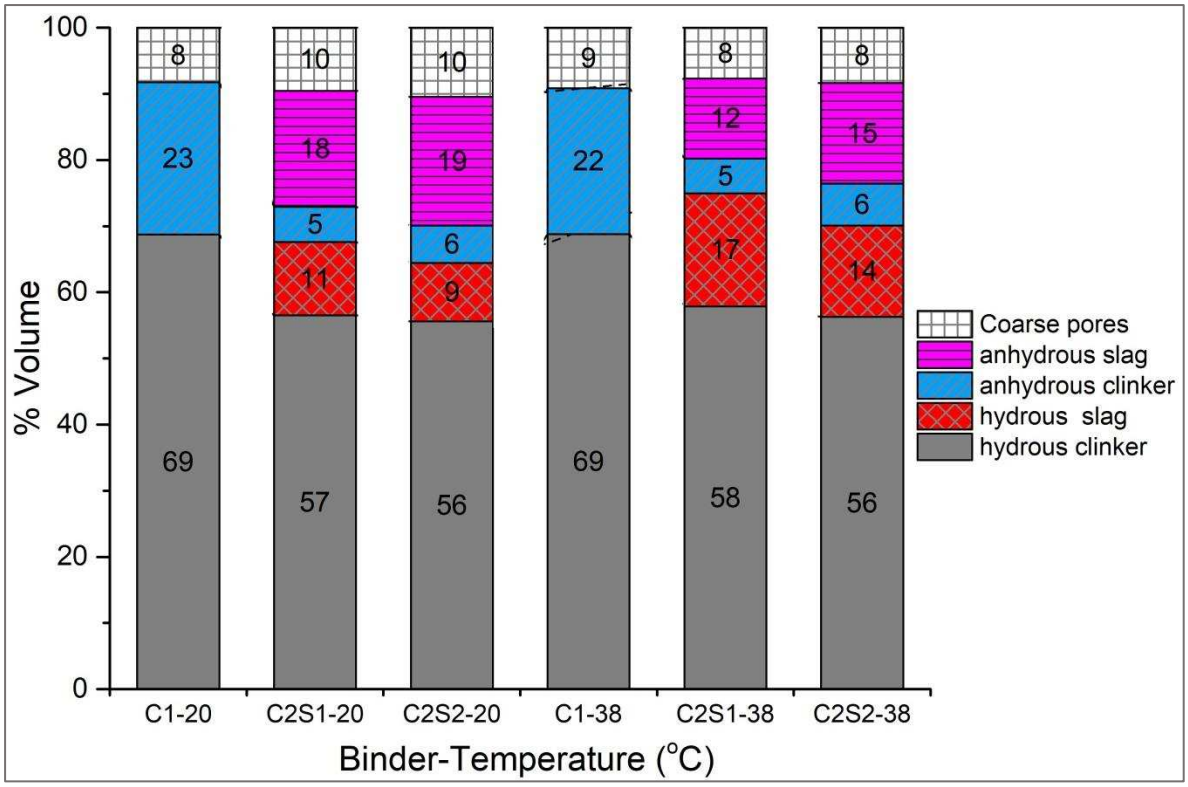

247

248 Figure 2: Hydrous and anhydrous clinker and slag contents for each binder at 7 days

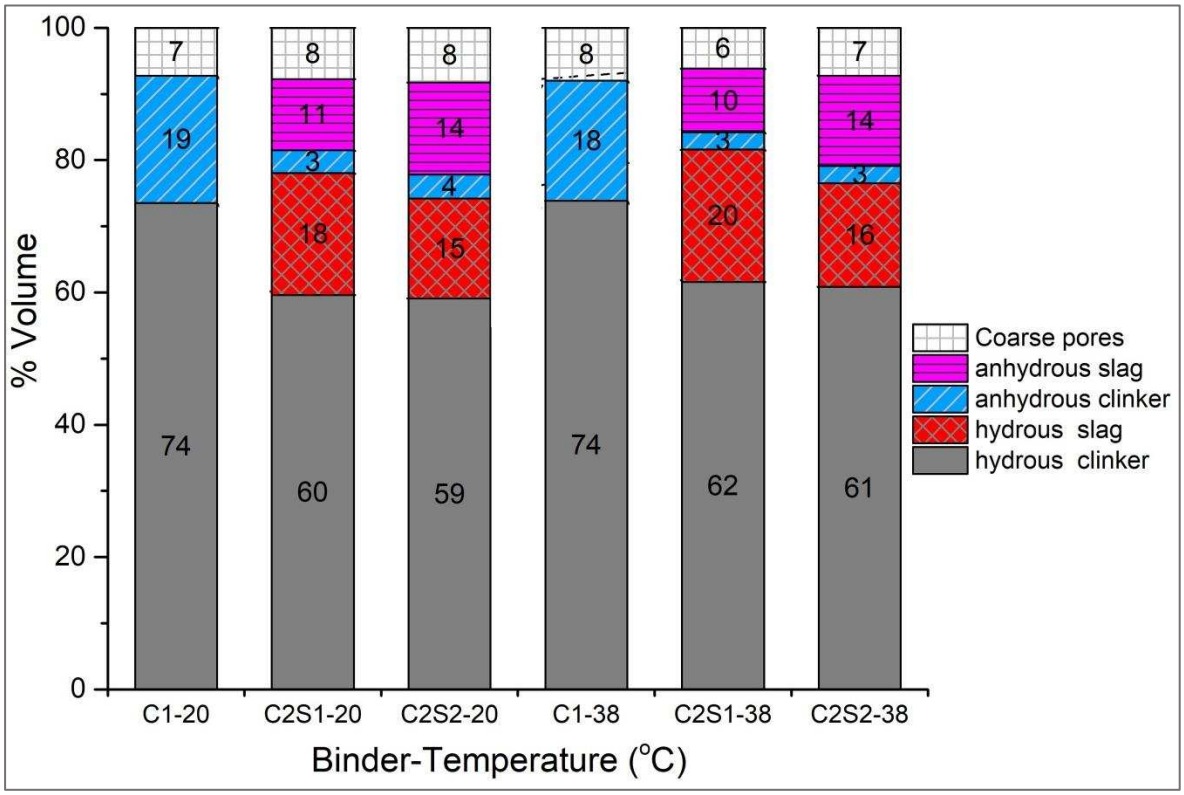

249

250 Figure 3: Hydrous and anhydrous clinker and slag contents for each binder at 28 days

Table 5: Weighted degrees of hydration as determined by SEM-IA

Age (day)	Mix	Degree of hydration (%) at 20℃				Degree of hydration (%) at 38℃			
		Slag	Clinker	Weighted	Error	Slag	Clinker	Weighted	Error
7	C1	-	74.9	74.9	0.74	-	75.8	75.8	1.02
	C2S1	38.7	91.3	75.6	0.80	58.6	91.7	81.8	0.50
	C2S2	31.3	90.8	73.0	0.99	47.6	89.9	77.2	0.79
28	C1	-	79.3	79.3	0.70	-	80.3	80.3	0.65
	C2S1	63.2	94.5	85.2	0.60	67.6	96.0	87.5	0.52
	C2S2	52.1	94.3	81.6	0.76	53.5	95.9	83.2	0.49
28X2	C1	0.0	79.5	79.5	0.40	0.0	82.6	82.6	0.87
	C2S1	64.3	95.0	85.8	0.44	69.4	96.4	88.3	0.58
	C2S2	54.5	95.6	83.3	0.60	57.2	97.1	85.2	0.49

Table 6: Capillary porosity (%) as determined by SEM-IA

Age (day)	Mix	20℃	Error	38℃	Error
7	C1	9.0	0.41	10.1	0.21
	C2S1	10.5	0.20	8.3	0.15
	C2S2	11.7	0.23	9.1	0.21
28	C1	7.8	0.09	8.7	0.11
	C2S1	8.4	0.20	6.6	0.12
	C2S2	9.0	0.13	7.8	0.14
28X2	C1	7.7	0.10	8.5	0.13
	30S1	8.2	0.13	7.1	0.14
	30S2	8.0	0.20	7.2	0.18

The extent of hydration was also probed by examining bound water contents, obtained from thermogravimetric analysis (TGA) and shown in Figure 4. Bound water contents increased generally from 7 to 28 days, indicating increasing hydration, consistent with SEM data presented earlier. Furthermore, there was generally an increased degree of hydration following exposure to the salt solution.

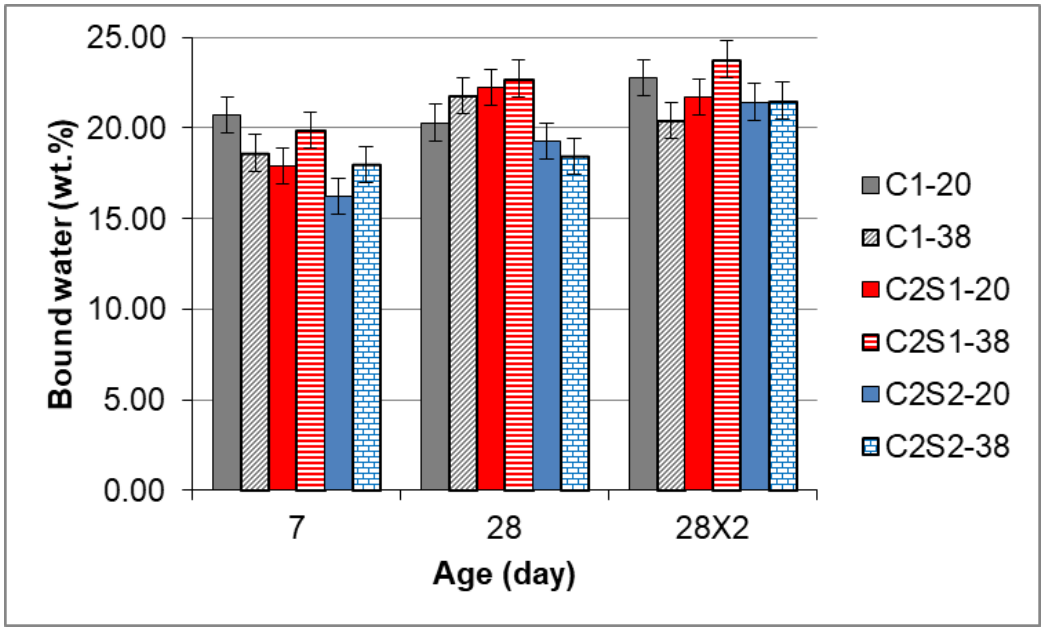

Figure 4: Bound water content from TGA (X2: specimens exposed to salt solution from 7 days, i.e. 28X2 refers to test age of 28days for specimens exposed to salt solution).

3.1.1 Evolution of hydration products from XRD

Figures 5 and 6 show XRD patterns obtained from specimens cured for 7 or 28 days at 20 and 38℃ respectively. The figures focus on the reflectio ns due to AFt and AFm phases. Before exposure to the salt solution, the main phases present in the CEM I pastes cured at 20℃ were ettringite and monocarboaluminate [48, 49] . The monocarboaluminate reflection increased from 7 to 28 days, while ettringite slightly converted to monosulfoaluminate.

Slag blends cured at 20℃ revealed lower ettringite le vels than did CEM I specimens, because higher aluminate contents led to increased monosulfoaluminate levels. Slag hydration also led to hydrotalcite formation [50, 51]. The monosulfoaluminate and hydrotalcite reflections increased with curing. Monosulfoaluminate and hydrotalcite reflections were more intense still for slag blends cured at 38℃. Furthermore, while dif ferences between the 2 slag blends were slight at 7 days, by 28 days when slag hydration had advanced significantly, monosulphate reflections were clearly more intense in the blend containing slag 1 than that containing slag 2, confirming the increased reactivity of slag 1, as shown by SEM data and bound water contents.

On exposure to salt solution, ettringite levels in the CEM I specimen increased, while monocarboaluminate converted to Friedel's salt (FS) [10, 21, 52]. Ettringite reflections were lower in the specimens cured for 28 days prior to exposure than for specimens cured for 7 days. This indicates reduced sulphate penetration due to a more refined microstructure, and reflects the reduced expansion observed (see later). Comparing 28 day old CEM I specimens between specimens cured in water and those exposed to the salt solution from 7 days shows intense reflections due to ettringite and Friedel's salt from the specimens exposed to salt solution. The reflections were also more intense at 38°C than 20°C. Hydration of CEM I is known to be activated at elevated temperature, but leads to a more porous microstructure [53, 54], allowing increased salt penetration. Hence, the higher levels of ettringite and Friedel's salt observed at 38℃.

Exposure of the slag blends to salt solution led to ettringite formation alongside the formation of Friedel's and Kuzel's salt. Kuzel's salt reflections were more intense at 38°C than 20°C. Monosulfoaluminate levels increased more significantly between 7 and 28 days for the more reactive, alumina-rich slag 1 than slag 2. This highlights the importance of slag composition on performance of blended cements, as shown by the different behaviours of slag 1 and 2 blends regarding the effects of curing duration at 20℃. As slag hydration was activated at the elevated temperature of 38℃, the 2 slag blends exposed to salt solutions displayed much more similar hydrate assemblages than at 20℃. Ettringite reflections decreased due to prolonged curing before exposure to salt solution, while reflections due to Friedel's salt were slightly diminished compared with specimens cured for only 7 days before exposure. These behaviours are consistent with the expansion behaviours of mortar prisms.

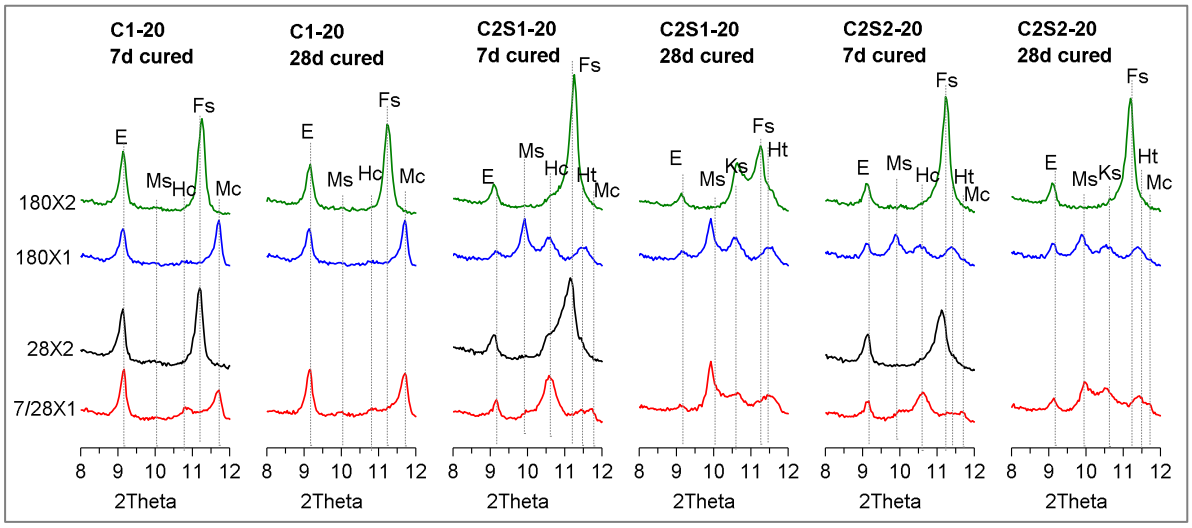

Figure 5: XRD patterns showing evolution AFt/AFm hydration products at 20℃.

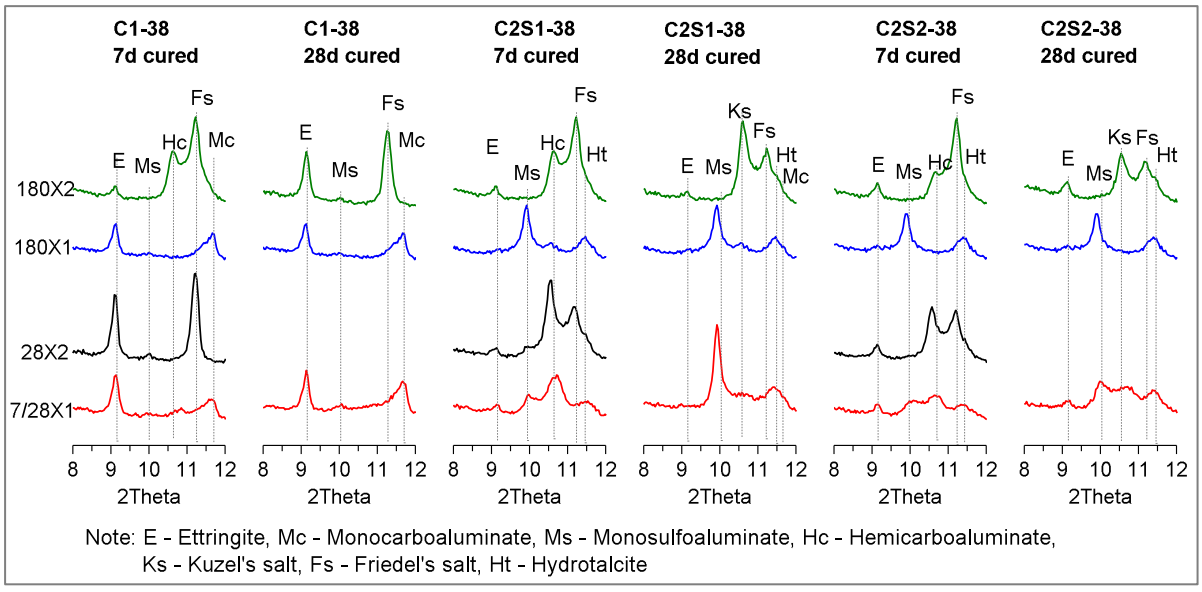

Figure 6: XRD patterns showing evolution AFt/AFm hydration products at 38℃.

3.1.2 Microstructure

Backscattered electron images are presented in Figures 7 and 8, showing the microstructures of binders hydrated for 7 and 28 days respectively. The diminished presence of bright, anhydrous particles confirmed that hydration was accelerated at elevated temperature for both slags and CEM I systems. This difference between the two curing temperatures was more noticeable at 7 days than at 28 days. With reference to the degrees of hydration reported in Table 5, each of the slag blends had hydrated faster than CEM I (C1), despite the retarding effects of slags on hydration of blends. This is due to the different cement used in the different mixes. The slag blends were prepared with CEM I 52.5R, as is common practice in industry. Increasing cement fineness is known to increase the rate of hydration [39, 55].

The micrographs showed increased presence of C-S-H from 7 to 28 days. The positive influence of elevated temperatures on slag hydration was marked by finer microstructures. Coarse porosity decreased upon hydration at 38℃ for the slag blends, in line with their more refined microstructures. Elevated temperature accelerated slag hydration, thus reducing the porosity by more than the increase in porosity induced by curing cement at higher temperatures. Conversely, coarse porosity increased for the CEM I specimens at elevated temperature, resulting in a more porous microstructure. This confirms earlier findings in the literature [53, 54], such that while hydration was accelerated, densification of the hydration products leads to increased porosity.

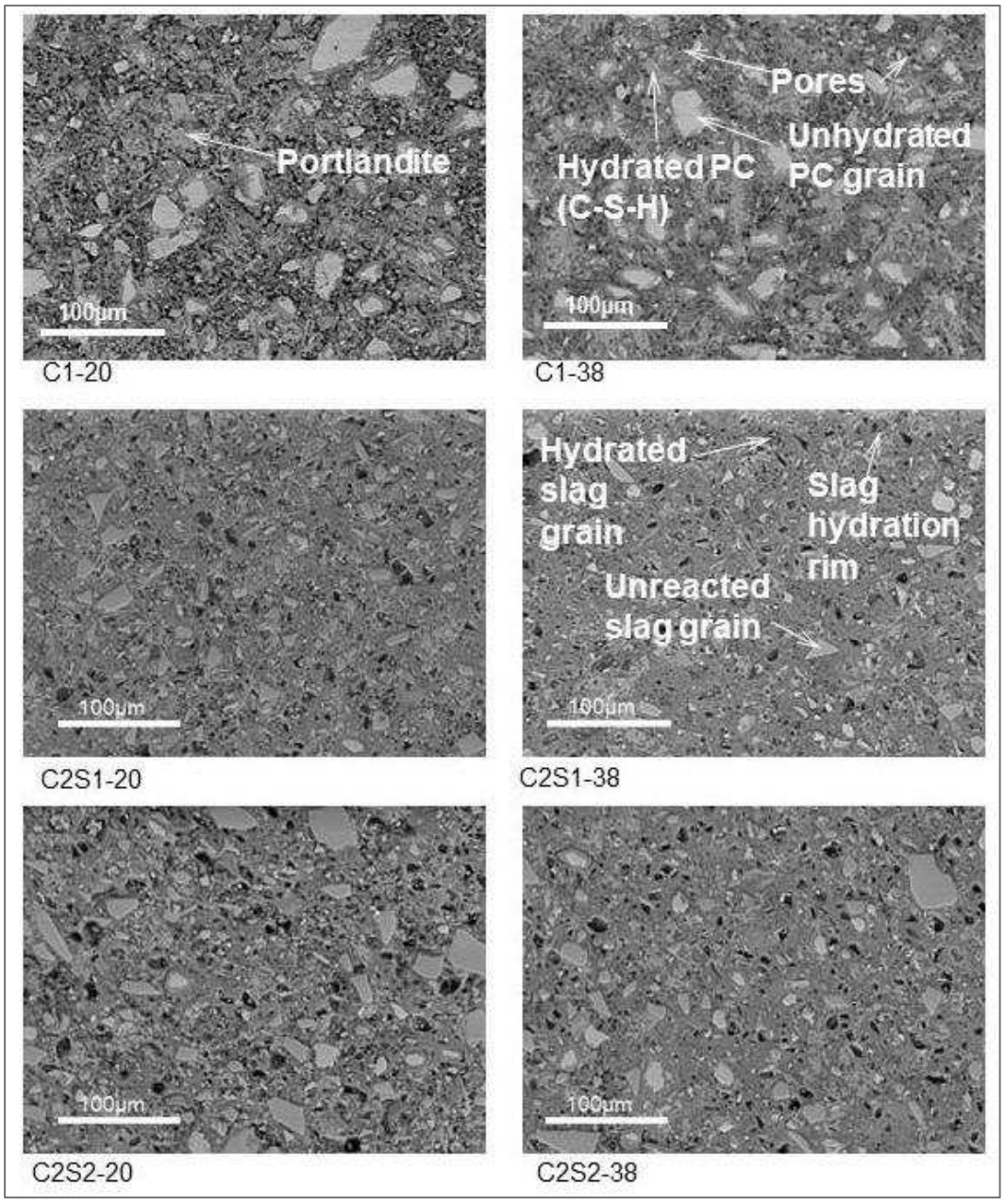

Figure 7: SEM-BSE micrographs of pastes hydrated for 7 days.

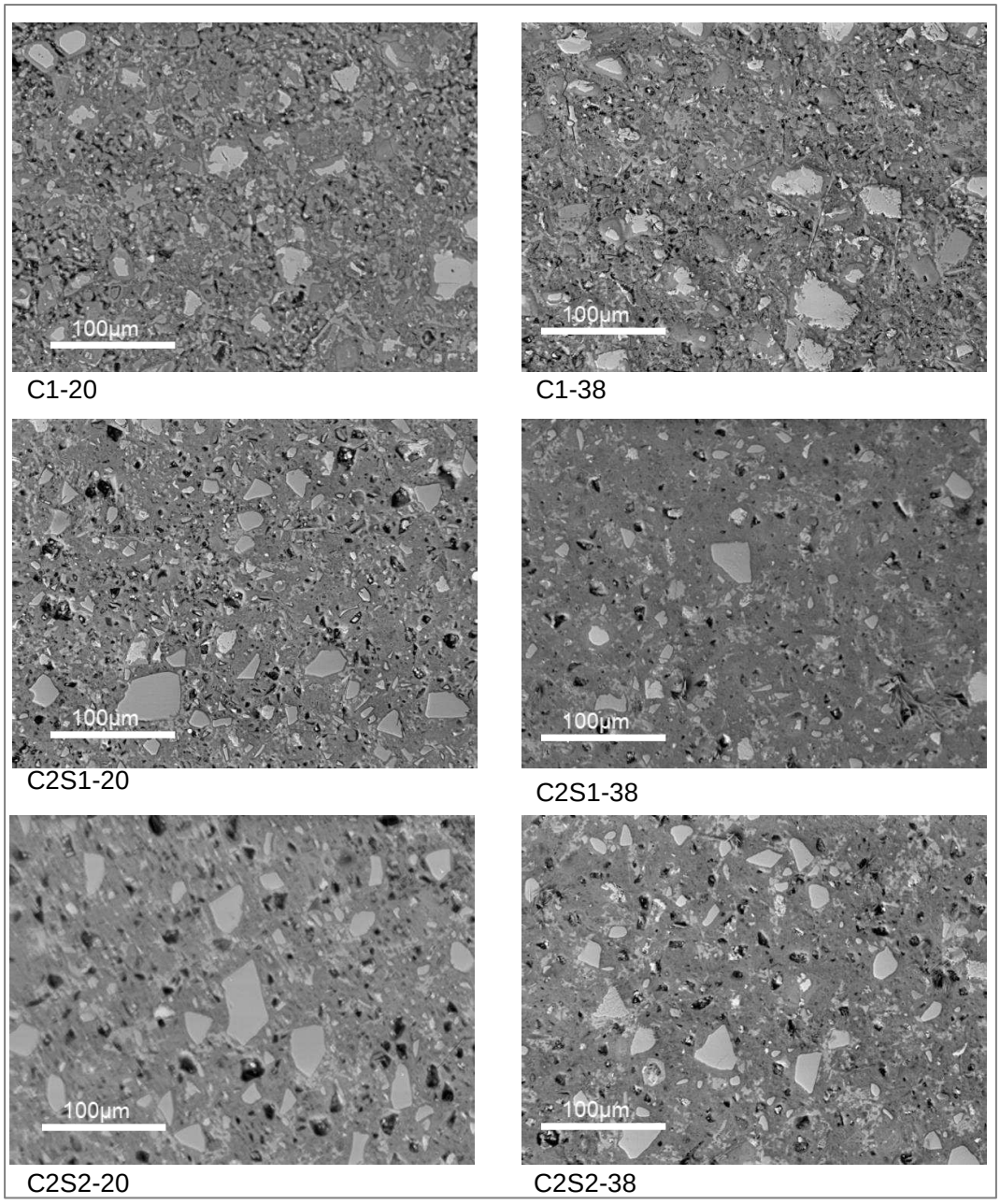

Figure 8: SEM-BSE micrographs of pastes hydrated for 28 days.

3.1.3 Sorptivity

Sorptivity coefficients were determined after 7 and 28 days, before exposure to salt solutions. The results are presented in Figures 9 and 10 for exposure at 20 and 38℃ respectively . In all cases, there was a reduction in sorptivity, in line with the reduction in coarse porosity as measured by image analysis, with prolonged hydration, irrespective of temperature. Similarly, sorptivity decreased when curing temperature was increased. Prolonged curing appeared more beneficial at 20^{o}C than at 38^{o}C, particularly for the slag blends. This was to be expected, where the degree of hydration showed similar behaviour (Table 5).

Sorptivity was also determined at 28 days for specimens that had been cured for 7 days prior to exposure to a salt solution. In all cases bar one, exposure to the salt solution led to a lower

sorptivity than curing alone. This can be attributed to increased silicate hydration in the presence of chlorides and the formation of Friedel's salt, Kuzel's salt and ettringite upon reaction of chloride and sulphate with hydrated aluminate phases (Figures 5 & 6). These new products tend to fill-up pore spaces, leading to reduced sorptivity as observed.

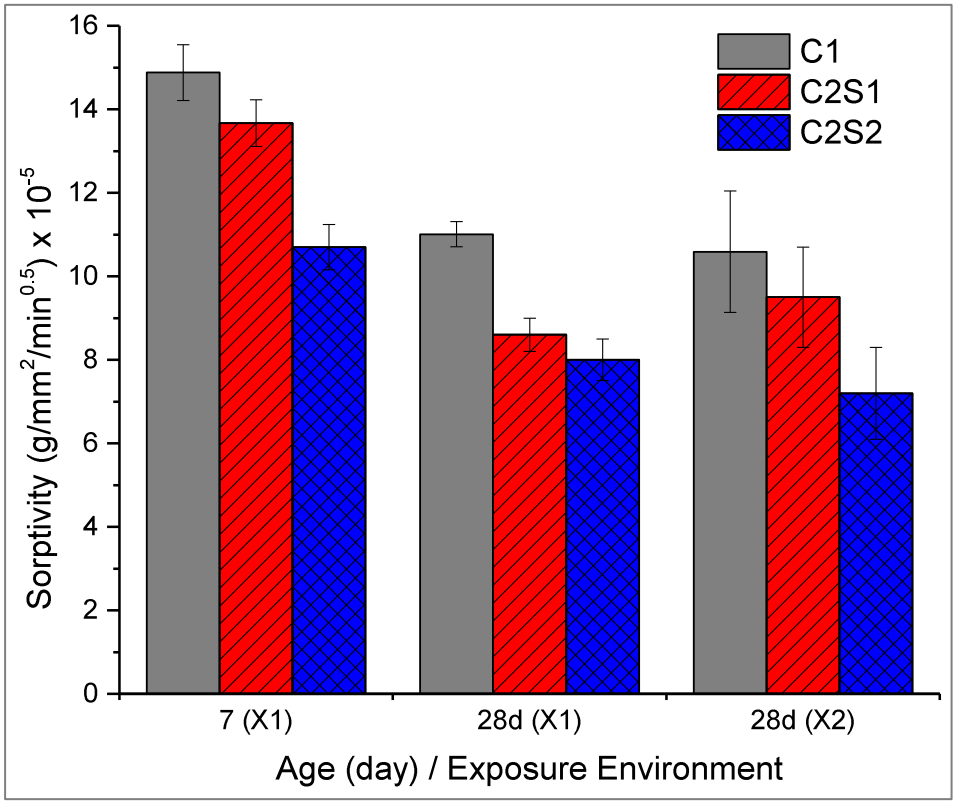

Figure 9: Sorptivity of specimens cured at 20℃.

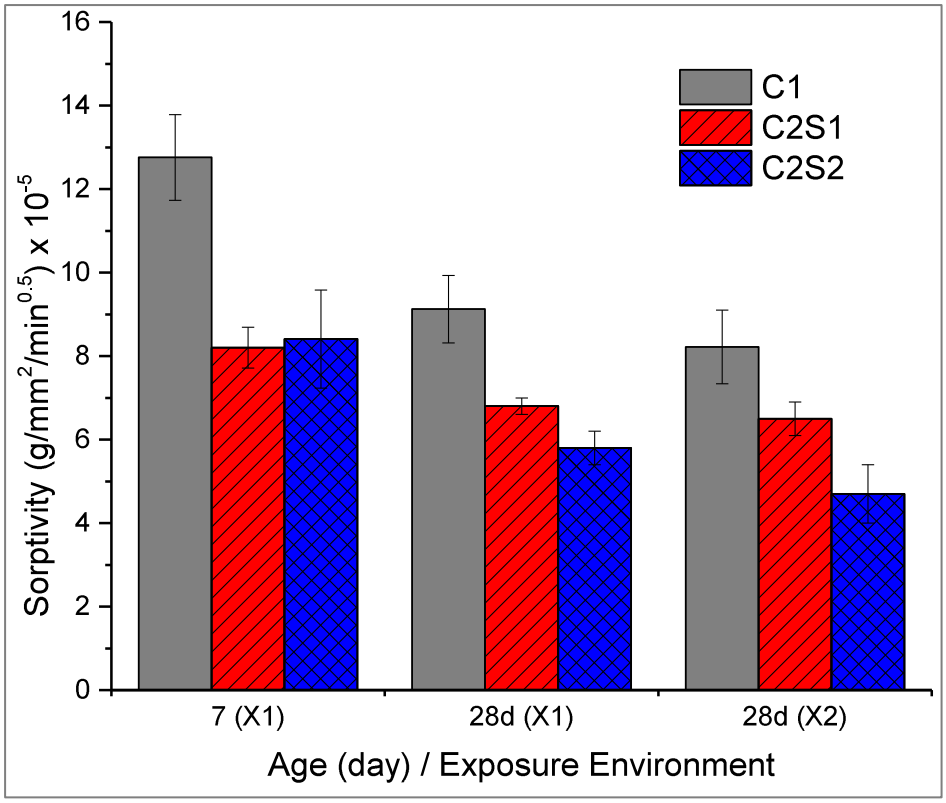

Figure 10: Sorptivity of specimens cured at 38℃.

3.2 Expansion of mortar prisms

Expansion results for each binder under different exposure conditions are presented in Figures 11, 12 and 13 for CEM I, slag 1 blend and slag 2 blend respectively.

Reference specimens submerged in limewater showed minimal dimensional change upon exposure for up to 664 days, suggesting that any expansion was due to salt ingress. It is now well accepted that expansion occurs in cement systems based on crystallisation pressure theory [5, 7, 8]. The nucleation and growth of ettringite crystals in small pore spaces can exert crystallisation pressures on the pore walls, leading to expansion.

In this study, temperature was the dominant factor, with expansion being significantly less for all mortars cured and exposed to salt solutions at 38℃ than at 20℃. This was the case for the CEM I systems, but was especially so for slag blends. Indeed, both slag blends, when cured at 38°C showed no expansion for the entire duration of the study whether cured for 7 or 28 days before exposure. This behaviour can be attributed to changes in the microstructure. The foregoing discussion also agrees with increase in flexural strengths reported for similar samples elsewhere [34], as increase in flexural strength will tend to improve the resistance towards internal stress development and reduce micro cracking. Ettringite decomposes at elevated temperatures greater than 50℃ [64, 65], the temperature used in this study is below this, and should not have any significant effect. As shown earlier, CEM I was more porous than the slag systems at elevated temperature, with the composite systems showing a dense, well-developed microstructure. Hence, there would have been greater ingress of the salts into the CEM I specimens. As expansion occurs due to the formation of ettringite exerting crystal pressures in confined pore spaces [5, 8], any increase in penetration of sulphate laden solution

can cause increased ettringite formation in the presence of hydrated aluminates, leading to more expansion.

For other situations, the situation was less clear cut. Generally, expansion was reduced in mortars which were cured for 28 days before exposure, irrespective of temperature. This is due to more refined microstructure after 28 days of hydration compared with 7 days. The only exception was the more reactive, alumina-rich slag 1 blend exposed at 20℃, which rather showed greater expansion after curing for 28 days than 7 days before exposure. This is contrary to the known positive influence of prolonged curing and the common practice of allocating longer curing durations for SCMs due to their slow hydration [46, 56-59]. However, it underscores the importance of considering the influence of slag composition in determining curing duration to prevent expansion in combined chloride-sulphate environments.

The above expansion behaviour of slag 1 blend may be explained by the slag's higher degree of hydration and the role of slag alumina content. Increasing slag alumina contents may cause slag blends to be more susceptible to sulphate attack. However, the alumina in slag is not readily available to react with the penetrating sulphate to form ettringite [11], but is incorporated in C-S-H and hydrotalcite-like phases during slag hydration, while the remainder converts slowly to monosulfoaluminate, which may subsequently react with the penetrating sulphate ions to form ettringite. However, expansion requires that the pore solution be supersaturated [1, 60-62]. Hence, at 7 days when the degree of slag hydration was still relatively low, there would be less alumina available to form monosulfoaluminate, compared with hydration at 28 days. The higher levels of monosulfoaluminate present after prolonged hydration, possibly, favoured more rapid ettringite formation, which led to the greater expansion observed. This is confirmed by the increasing level of monosulfoaluminate formed between 7 and 28 days, as observed by XRD analysis (Figure 5). Slag 2 behaved slightly differently due to microstructural changes and slag composition. Both the CEM I and slag 2 specimens showed greater expansion after curing for 7 days before exposure. This can be attributed to their more porous microstructure compared with the slag 1 blend, as shown by the capillary porosity discussed earlier.

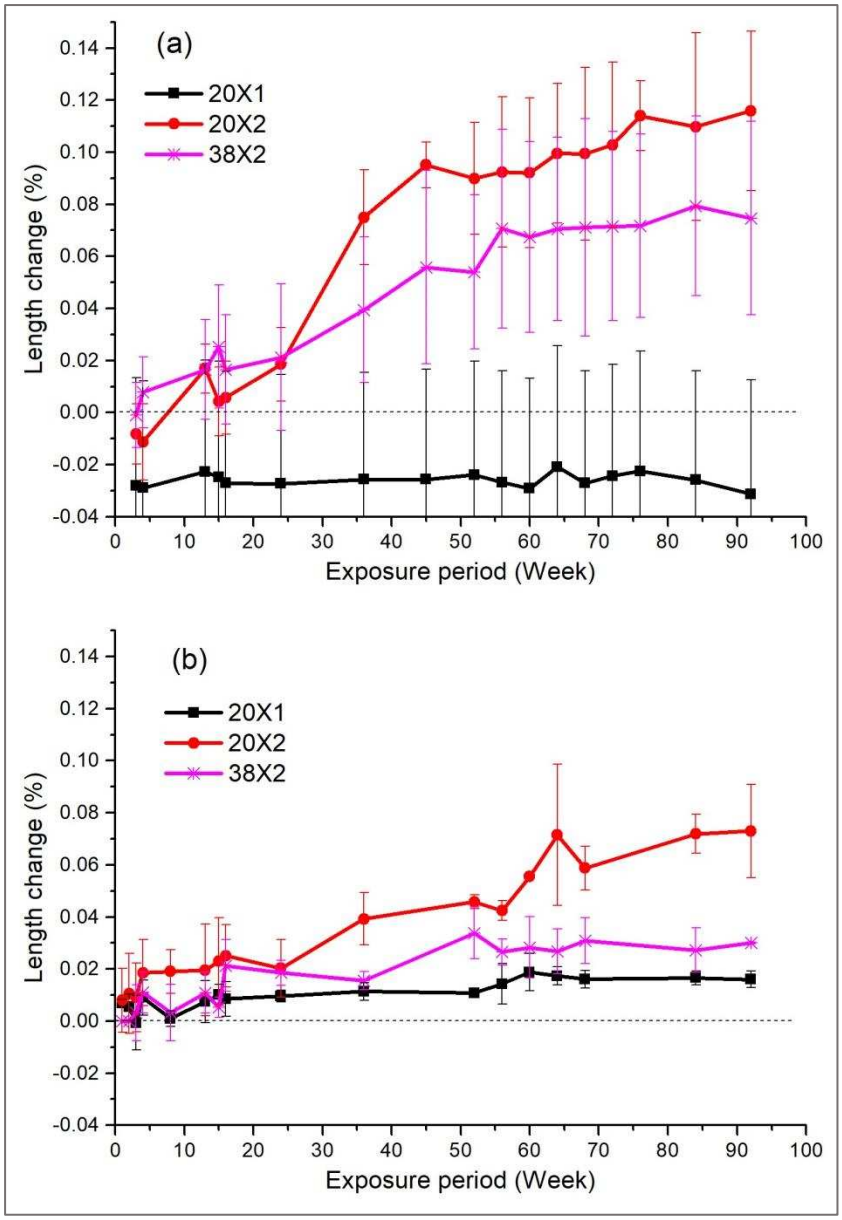

Figure 11: Length-change/expansion of CEM I: (a) cured for 7 days, (b) cured for 28 days, before exposure.

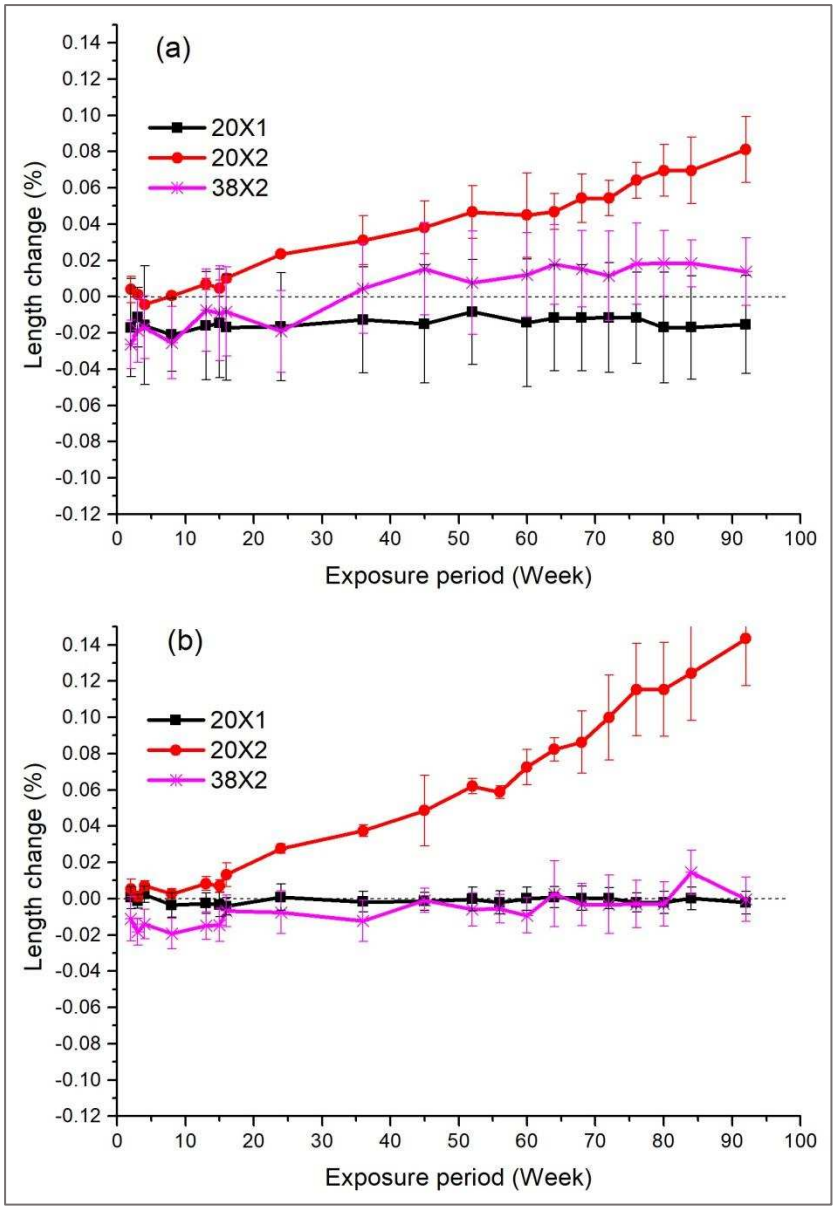

Figure 12: Length-change/expansion of slag 1 blend: (a) cured for 7 days, (b) cured for 28 days, before exposure.

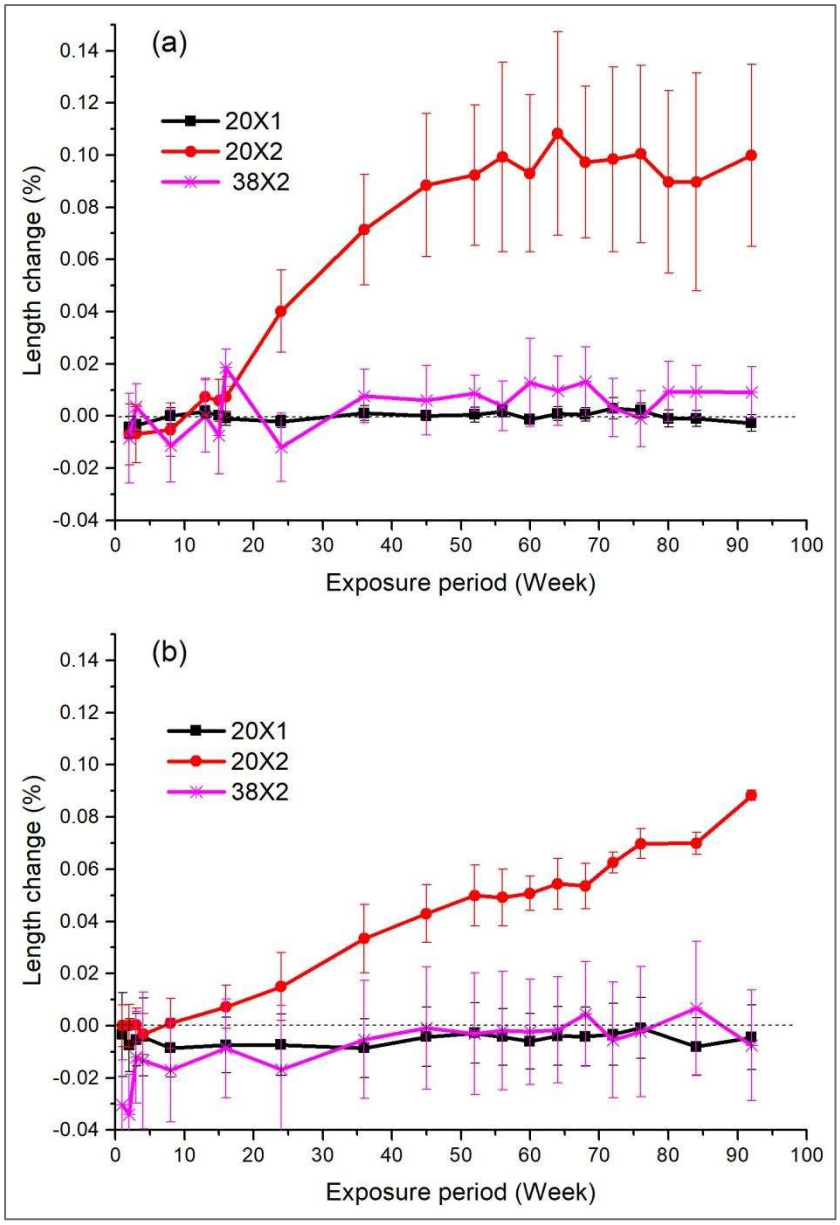

Figure 13: Length-change/expansion of slag 2 blend: (a) cured for 7 days, (b) cured for 28 days, before exposure.

3.2.1 Influence of chloride presence and slag contents on expansion

The influence of the presence of chloride on sulphate expansion is observed in Figure 14, showing comparison between expansion of CEM I in pure sulphate [40] and a combined chloride-sulphate solution. Expansion was similar in the 2 media until about 55 weeks, where the mitigating role of chloride on sulphate attack became evident. This is consistent with the literature [20, 21, 63]. It must be noted that similar specimens, sulphate concentrations and conditions were used in the present study as in [40].

Generally, the interactions of ions in complex solutions seem to reduce the effects of attack in comparison to single salt solution [7, 10]. This is due to increased solubility of ettringite in chloride solution [66, 67] with reduced impact on crystallization pressure.

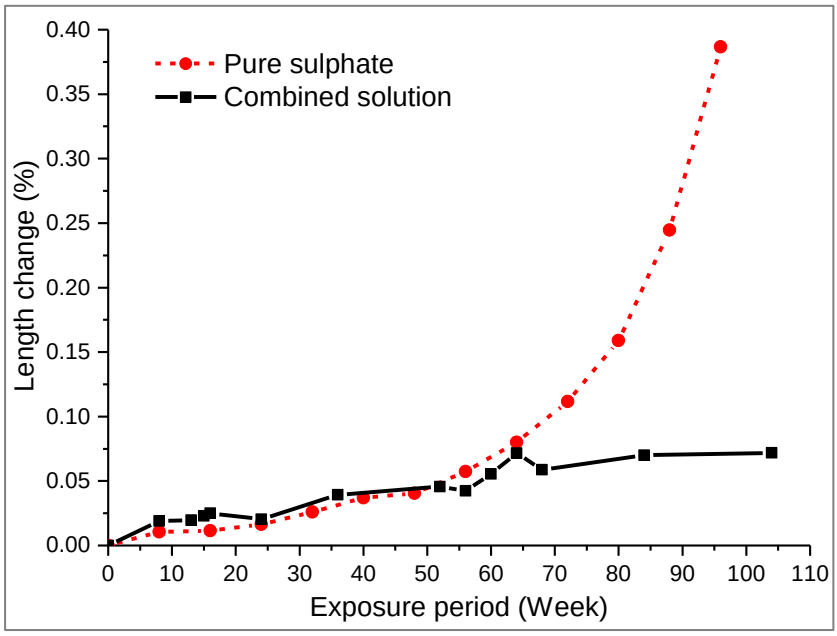

Figure 14: Comparison between expansion of CEM I in pure sulphate and combined chloride-sulphate solutions (Pure sulphate data taken from Whittaker [40]).

3.3 Visual observation

Specimens were examined visually, with Figure 15 showing mortar prisms immersed in saturated lime water (X1) and combined chloride-sulphate solution (X2) pre-cured for 7 and 28 days. No significant macro cracks were visible within the period of this study. However, slight surface loss was observed in both reference and test specimens, which may be related to the activity of water continuously present in the specimens, rather than sulphate attack. This is particularly so since similar observations were made on reference specimens which were stored in saturated lime water. No trend could yet be established linking expansion with the surface losses or popouts observed in various test specimens subjected to different conditions. At a similar exposure period, Whittaker [40] observed significant macro cracks in similar CEM I mortar prisms immersed in a pure sulphate solution. This difference further confirms the mitigating role of chloride on sulphate-oriented expansion and damage in cementitious materials, consistent with the literature [20-22].

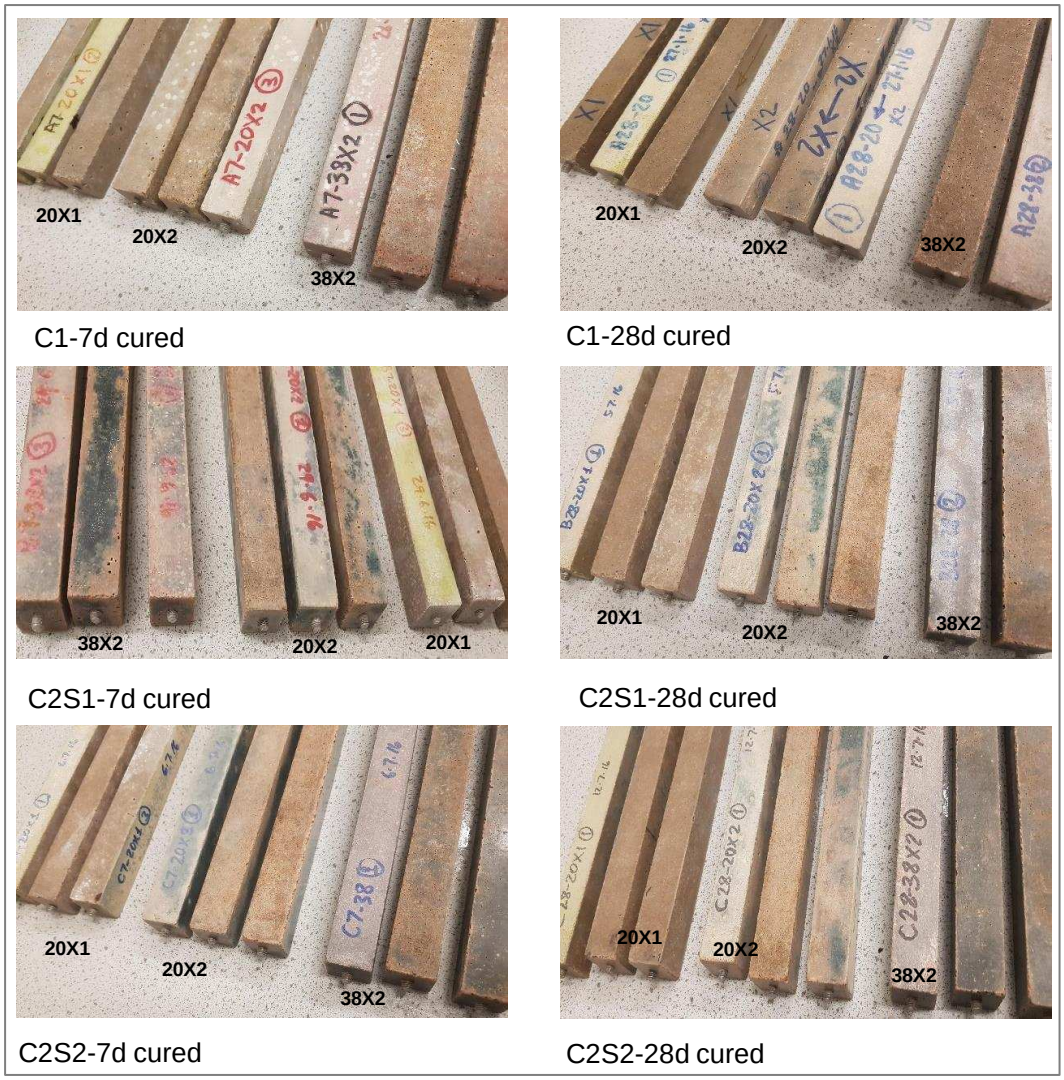

462

463 Figure 15: Visual appearance of CEM I and slag blends exposed to lime water (X1) and salt
464 water (X2) after 664 days.

465

466 **4.0 Conclusions**

467 The expansion and sulphate-oriented damage of CEM I and slag-blended cement mortars
468 exposed to combined chloride-sulphate solutions has been investigated under various
469 conditions, supplemented by microstructural characterisation and determination of specimen
470 transport properties prior to exposure. The results highlight important effects of temperature,
471 curing duration and slag composition on sulphate attack of CEM I and slag blends, including
472 the influence of chloride presence on sulphate attack of CEM I.

473 Resistance to sulphate attack was significantly improved by curing and exposing slag blend
474 mortar prisms at 38℃. This behaviour was attributed to accelerated slag hydration at elevated
475 temperature, leading to more refined microstructures and greatly decreased penetration of the
476 salt solution. The slag specimens showed approximately no expansion irrespective of curing
477 duration, indicating that prolonged curing beyond 7 days, when specimens are exposed within
478 climates having such elevated temperature seemed unnecessary. Hence, the costs and time
479 losses associated with prolonged curing when these slags are used may thus be saved. This

finding is significant for the practical application of these slag blends to control combined chloride-sulphate attack in warm tropical climates.

At 20℃, however, prolonged curing becomes important, although the influence of slag composition must be considered carefully. This study has shown that shorter curing periods are not too problematic in terms of expansion, but there is increased chloride penetration. Nevertheless, the less reactive slag 2, with lower alumina content, showed improved resistance to sulphate expansion as a result of prolonged curing duration, consistent with the behaviour of CEM I. This finding has highlighted the importance of considering slag composition and curing/exposure conditions if the desired performance of slag blends must be achieved. This study has highlighted the influence of slag composition, and particularly, the role of alumina contents of slags, regarding curing duration in combined chloride-sulphate aggressive environments to enhance proper application and durability of structures incorporating slag blends.

Acknowledgements

The authors gratefully acknowledge the support of Niger Delta Development Commission (NDDC), Nigeria for providing the PhD scholarship for this research.

References

[1] J. Skalny, J. Marchand, I. Odler, Sulfate Attack on Concrete, 1st ed., Spon Press, London, 2002.
[2] M. Whittaker, L. Black, Current knowledge of external sulfate attack, Adv. Cem. Res. 27(9) (2015) 532-545.
[3] G.W. Scherer, Stress from crystallization of salt, Cem. Concr. Res. 34(9) (2004) 1613-1624.
[4] R.J. Flatt, G.W. Scherer, Thermodynamics of crystallization stresses in DEF, Cem. Concr. Res. 38(3) (2008) 325-336.
[5] C. Yu, W. Sun, K. Scrivener, Mechanism of expansion of mortars immersed in sodium sulfate solutions, Cem. Concr. Res. 43 (2013) 105-111.
[6] G.W. Scherer, Crystallization in pores, Cem. Concr. Res. 29(8) (1999) 1347-1358.
[7] W. Kunther, B. Lothenbach, K.L. Scrivener, On the relevance of volume increase for the length changes of mortar bars in sulfate solutions, Cem. Concr. Res. 46 (2013) 23-29.
[8] W. Müllauer, R.E. Beddoe, D. Heinz, Sulfate attack expansion mechanisms, Cem. Concr. Res. 52 (2013) 208-215.
[9] C. Yu, W. Sun, K. Scrivener, Degradation mechanism of slag blended mortars immersed in sodium sulfate solution, Cem. Concr. Res. 72 (2015) 37-47.
[10] M. Maes, N. De Belie, Resistance of concrete and mortar against combined attack of chloride and sodium sulphate, Cem. Concr. Compos. 53 (2014) 59-72.
[11] M. Whittaker, M. Zajac, M. Ben Haha, L. Black, The impact of alumina availability on sulfate resistance of slag composite cements, Constr. Build. Mater. 119 (2016) 356-369.
[12] A.M. Hossack, M.D.A. Thomas, Varying fly ash and slag contents in Portland limestone cement mortars exposed to external sulfates, Constr. Build. Mater. 78(0) (2015) 333-341.
[13] S. Ogawa, T. Nozaki, K. Yamada, H. Hirao, R.D. Hooton, Improvement on sulfate resistance of blended cement with high alumina slag, Cem. Concr. Res. 42(2) (2012) 244-251.
[14] M. Santhanam, M.D. Cohen, J. Olek, Mechanism of sulfate attack: a fresh look: Part 2. Proposed mechanisms, Cem. Concr. Res. 33(3) (2003) 341-346.

[15] A. Fatemeh, R.D. Hooton, Sulfate Resistance of Portland and Slag Cement Concretes Exposed to Sodium Sulfate for 38 Years, Materials Journal 114(3) (2017) 477-490.
[16] W. Kunther, B. Lothenbach, J. Skibsted, Influence of the Ca/Si ratio of the C–S–H phase on the interaction with sulfate ions and its impact on the ettringite crystallization pressure, Cem. Concr. Res. 69 (2015) 37-49.
[17] A.M. Hossack, M.D.A. Thomas, Evaluation of the effect of tricalcium aluminate content on the severity of sulfate attack in Portland cement and Portland limestone cement mortars, Cem. Concr. Compos. 56(0) (2015) 115-120.
[18] C. Ouyang, A. Nanni, W.F. Chang, Internal and external sources of sulfate ions in portland cement mortar: two types of chemical attack, Cem. Concr. Res. 18(5) (1988) 699-709.
[19] M. Santhanam, M. Cohen, J. Olek, Differentiating seawater and groundwater sulfate attack in Portland cement mortars, cement & Concrete Research 36(2006) (2006) 2132-2137.
[20] G. Li, A. Zhang, Z. Song, S. Liu, J. Zhang, Ground granulated blast furnace slag effect on the durability of ternary cementitious system exposed to combined attack of chloride and sulfate, Constr. Build. Mater. 158 (2018) 640-648.
[21] S.-T. Lee, D.-W. Park, K.-Y. Ann, Mitigating effect of chloride ions on sulfate attack of cement mortars with or without silica fume, Canadian Journal of Civil Engineering 35(1) (2008) 1210-1220.
[22] M. Zhang, J. Chen, Y. Lv, D. Wang, J. Ye, Study on the expansion of concrete under attack of sulfate and sulfate–chloride ions, Constr. Build. Mater. 39 (2013) 26-32.
[23] M. Maes, N. De Belie, Influence of chlorides on magnesium sulphate attack for mortars with Portland cement and slag based binders, Constr. Build. Mater. 155 (2017) 630-642.
[24] O.S.B. Al-Amoudi, Mechanisms of Sulfate Attack in Plain and Blended Cements- A Review, Extending performance of concrete structures, International congress "creating with concrete", Dundee, 1999, pp. 247-260.
[25] O.S.B. Al-Amoudi, Attack on plain and blended cements exposed to aggressive sulphate environments, Cement & Concrete Composites 24(1) (2002) 305-316.
[26] A.M. Hossack, M.D.A. Thomas, The effect of temperature on the rate of sulfate attack of Portland cement blended mortars in Na2SO4 solution, Cem. Concr. Res. 73 (2015) 136-142.
[27] K. Sotiriadis, E. Nikolopoulou, S. Tsivilis, A. Pavlou, E. Chaniotakis, R.N. Swamy, The effect of chlorides on the thaumasite form of sulfate attack of limestone cement concrete containing mineral admixtures at low temperature, Constr. Build. Mater. 43(0) (2013) 156-164.
[28] A. Abdalkader, C. Lynsdale, J. Cripps, Corrosion behaviour of steel rebar in mortars subjected to magnesium sulfate and sodium chloride mixtures at 5 and 20°C, Constr. Build. Mater. 153 (2017) 358-363.
[29] A.H.M. Abdalkader, C.J. Lynsdale, J.C. Cripps, The effect of chloride on cement mortar subjected to sulfate exposure at low temperature, Constr. Build. Mater. 78(0) (2015) 102-111.
[30] F. Abubaker, C. Lynsdale, J. Cripps, Investigation of concrete–clay interaction with regards to the thaumasite form of sulfate attack, Constr. Build. Mater. 67, Part A(0) (2014) 88-94.
[31] C. Shi, D. Wang, A. Behnood, Review of Thaumasite Sulfate Attack on Cement Mortar and Concrete, J. Mater. Civ. Eng. 24(12) (2012) 1450-1460.
[32] F. Aköz, F. Türker, S. Koral, N. Yüzer, Effects of raised temperature of sulfate solutions on the sulfate resistance of mortars with and without silica fume, Cem. Concr. Res. 29(4) (1999) 537-544.
[33] M. Santhanam, M.D. Cohen, J. Olek, Modeling the effects of solution temperature and concentration during sulfate attack on cement mortars, Cem. Concr. Res. 32(4) (2002) 585-592.
[34] J.O. Ukpata, P.A.M. Basheer, L. Black, Performance of plain and slag-blended cements and mortars exposed to combined chloride–sulfate solution, Adv. Cem. Res. 30(8) (2018) 371-386.
[35] O.R. Ogirigbo, Influence of Slag Composition and Temperature on the Hydration and Performance of Slag Blends in Chloride Environments, School of Civil Engineering, The University of Leeds, 2016.
[36] K.L. Scrivener, B. Lothenbach, N. De Belie, E. Gruyaert, J. Skibsted, R. Snellings, A. Vollpracht, TC 238-SCM: hydration and microstructure of concrete with SCMs, Mater. Struct. 48(4) (2015) 835-862.

[37] M. Whittaker, M. Zajac, M. Ben Haha, F. Bullerjahn, L. Black, The role of the alumina content of slag, plus the presence of additional sulfate on the hydration and microstructure of Portland cement-slag blends, Cem. Concr. Res. 66 (2014) 91-101.
[38] V. Kocaba, E. Galluci, K.L. Scrivener, Methods for the determination of degree of reaction of slag in blended cement pastes, Cement & Concrete Research 42 (2012) 511-525.
[39] K.L. Scrivener, Backscattered electron imaging of cementitious microstructures: understanding and quantification, Cem. Concr. Compos. 26(8) (2004) 935-945.
[40] M.J. Whittaker, The Impact of Slag Composition on the Microstructure of Composite Slag Cements Exposed to Sulfate Attack, School of Civil Engineering, University of Leeds, Leeds, 2014, p. 253.
[41] BS EN 13057, Products and systems for the protection and repair of concrete structures — Test methods — Determination of resistance of capillary absorption, BSI, 2002.
[42] E. Guneyisi, M. Gesoglu, A study on durability properties of high-performance concretes incorporating high replacement levels of slag, Mater. Struct. 41 (2008) 479–493.
[43] B.B. Sabir, S. Wild, M. O'Farrell, A water sorptivity test for mortar and concrete, Materials and Structures/Materiaux et Constructions 31(1) (1998) 568-574.
[44] ASTM C1012, Annual Book of the ASTM standards, Standard test method for length change of hydraulic-cement mortars exposed to sulfate solution, ASTM International, United States, 2013, pp. 539-543.
[45] I. Galan, F.P. Glasser, Chloride in cement, Adv. Cem. Res. 27(2) (2015) 63-97.
[46] O.R. Ogirigbo, J.O. Ukpata, Effect of Chlorides and Curing Duration on the Hydration and Strength Development of Plain and Slag Blended Cements, Journal of Civil Engineering Research 7(1) (2017) 9-16.
[47] S. Adu-Amankwah, L. Black, J. Skocek, M. Ben Haha, M. Zajac, Effect of sulfate additions on hydration and performance of ternary slag-limestone composite cements, Constr. Build. Mater. 164 (2018) 451-462.
[48] T. Matschei, B. Lothenbach, F.P. Glasser, The AFm phase in Portland cement, Cem. Concr. Res. 37(2) (2007) 118-130.
[49] A. Ipavec, R. Gabrovgek, T. Vuk, V. KauWiW, J. MaWek, A. Medenz, Carboaluminate Phases Formation During the Hydration of Calcite-Containing Portland Cement, J. Am. Ceram. Soc. 94(4) (2011) 1238-1242.
[50] Y. Elakneswaran, E. Owaki, S. Miyahara, M. Ogino, T. Maruya, T. Nawa, Hydration study of slag-blended cement based on thermodynamic considerations, Constr. Build. Mater. 124 (2016) 615-625.
[51] P.T. Durdziński, M. Ben Haha, M. Zajac, K.L. Scrivener, Phase assemblage of composite cements, Cem. Concr. Res. 99 (2017) 172-182.
[52] J. Stroh, B. Meng, F. Emmerling, Deterioration of hardened cement paste under combined sulphate-chloride attack investigated by synchrotron XRD, Solid State Sciences 56 (2016) 29-44.
[53] J.I. Escalante-García, J.H. Sharp, Effect of temperature on the hydration of the main clinker phases in portland cements: part i, neat cements, Cem. Concr. Res. 28(9) (1998) 1245-1257.
[54] B. Lothenbach, F. Winnefeld, C. Alder, E. Wieland, P. Lunk, Effect of temperature on the pore solution, microstructure and hydration products of Portland cement pastes, Cem. Concr. Res. 37 (2007) 483-491.
[55] M.M.C. Fernandez, Effect of Particle Size on the Hydration Kinetics and Microstructural Development of Tricalcium Silicate, Laboratoire des Matériaux de Construction, École Polytechnique Fédérale de Lausanne, Suisse, 2008, p. 199.
[56] BS 6349-4, Maritime works, Part 1-4: General – Code of practice for materials, British Standard Institution, London, 2013.
[57] N. Gowripalan, J.G. Cabrera, A.R. Cusens, P.J. Wainwright, Effect of Curing on Durability, Concr. Int. 12(2) (1990).
[58] O. Idowu, L. Black, The effect of improper curing on properties that may affect concrete durability, Magazine of Concrete Research 70(12) (2018) 633-647.

[59] O.R. Ogirigbo, L. Black, The effect of slag composition and curing duration on the chloride ingress resistance of slag blended cements, Adv. Cem. Res. 31(5), 2019, 243-250.
[60] R.S. Gollop, H.F.W. Taylor, Microstructural and microanalytical studies of sulfate attack. II. Sulfate-resisting Portland cement: Ferrite composition and hydration chemistry, Cem. Concr. Res. 24(7) (1994) 1347-1358.
[61] R.S. Gollop, H.F.W. Taylor, Microstructural and microanalytical studies of sulfate attack. I. Ordinary portland cement paste, Cem. Concr. Res. 22(6) (1992) 1027-1038.
[62] R.S. Gollop, H.F.W. Taylor, Microstructural and microanalytical studies of sulfate attack. IV. Reactions of a slag cement paste with sodium and magnesium sulfate solutions, Cem. Concr. Res. 26(7) (1996) 1013-1028.
[63] F. Shaheen, B. Pradhan, Influence of sulfate ion and associated cation type on steel reinforcement corrosion in concrete powder aqueous solution in the presence of chloride ions, Cem. Concr. Res. 91 (2017) 73-86.
[64] A. Jimenez, M. Prieto, Thermal Stability of Ettringite Exposed to Atmosphere: Implications for the Uptake of Harmful Ions by Cement, Environ. Sci. Technol. 49(13) (2015) 7957-7964.
[65] B. Lothenbach, P. Durdziński, K.D. Weerdt, Thermogravimetric analysis, in: K. Scrivener, R. Snellings, B. Lothenbach (Eds.), A practical Guide to Microstructural Ananlysis of Cementitious Materials, CRC Press, Taylor and Francis Group, London, 2016, pp. 177-212.
[66] K.M.A. Hossain, Performance of volcanic ash and pumice-based blended cements in sulphate and sulphate - chloride environments, Adv. Cem. Res. 18 (2006) 71-82.
[67] S. Mindess, J.F. Young, D. Darwin, Concrete, 2 ed., Prentice Hall, United States, 2002.